Chapter 3

Dynamics of Random Packings[1]

3.1 Introduction

In the previous chapter, it was shown that the spot model can provide a reasonable mathematical model of mean flow and particle motion in granular drainage. However, since particles are off-lattice, and there is nothing to prevent them from overlapping, it quickly generates unphysical packings.

One of the primary motivations of the spot model comes from a consideration of the local packing geometry, and it would therefore be advantageous if the spot model could be refined to correctly simulate the local packing rearrangements. We therefore proposed the model shown in figure 3-2, whereby each spot-induced block displacement (a) is followed by a relaxation step (b), in which the affected particles and their nearest neighbors experience a soft-core repulsion (with all other particles held fixed). The net displacement in (c) involves a cooperative local deformation, whose mean is roughly the block motion in (a). It is not clear *a priori* that this procedure can produce realistic flowing packings, and, if so, whether the relaxation step dominates the simple dynamics from the original model.

To answer these questions, we calibrated and tested the spot model against a large-scale DEM simulation of granular drainage, shown in figure 3-1. Simulations are

[1]This chapter is based on reference [112], *Dynamics of Random Packings in Granular Flow*, published in Physical Review E in 2006. See `http://pre.aps.org/` for more details.

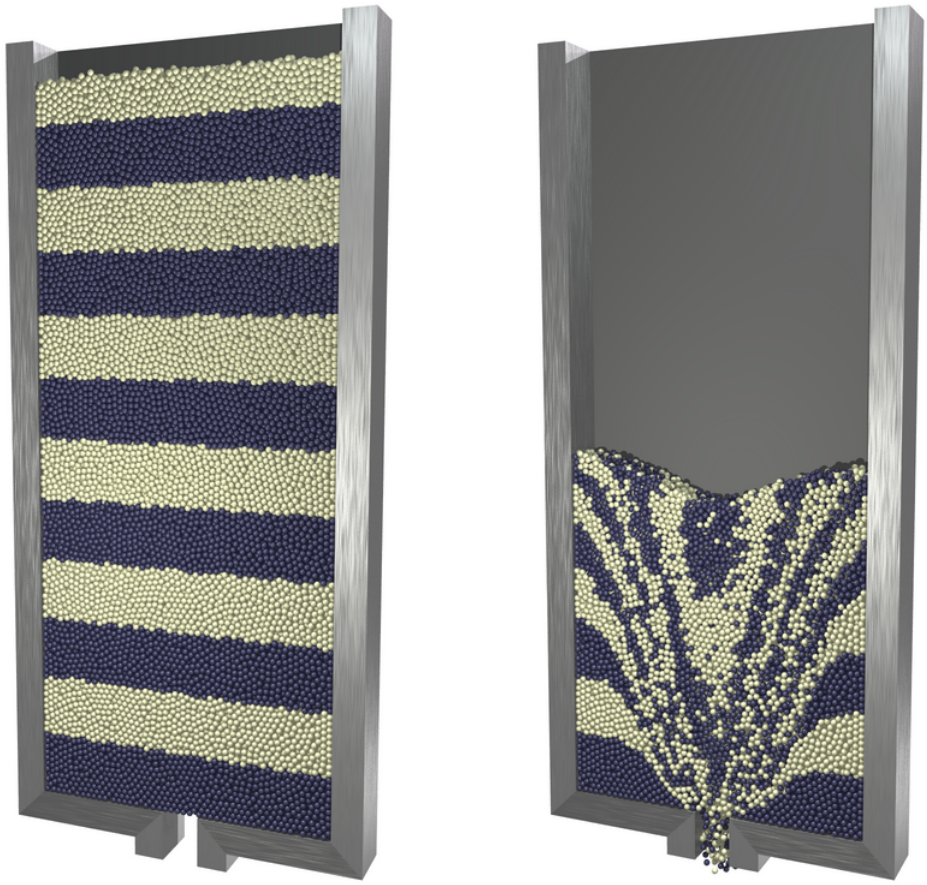

(a) (b)

Figure 3-1: A simulation of the experiment in Ref. [28] by discrete element simulations. (a) First, 55,000 glass beads are poured into a quasi-two-dimensional silo (8 beads deep) and let come to rest. (b) Slow drainage occurs after a slit orifice is opened. (The grains are identical, but colored by their initial height.)

advantageous in this case since three-dimensional packing dynamics cannot easily be observed experimentally. We begin by running the DEM simulation, briefly described in section 3.2. We then calibrate the free parameters in the spot model by measuring various statistical quantities from the DEM simulation, as described in 3.3. In section 3.4, we describe the computational implementation of the spot model, before carrying out a detailed comparison to DEM in section 3.5.

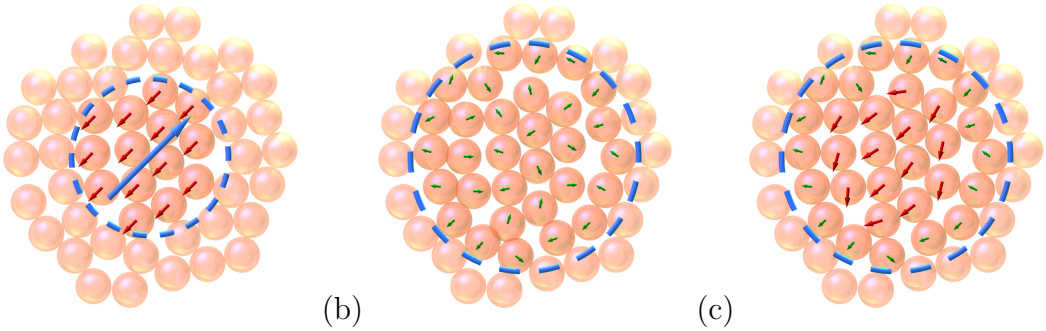

Figure 3-2: The mechanism for structural rearrangement in the spot model. The random displacement $\mathbf{r}_s$ of a diffusing spot of free volume (dashed circle) causes affected particles to move as a block by an amount $\mathbf{r}_p$ (a), followed by an internal relaxation with soft-core repulsion (b), which yields the net cooperative motion (c). (The displacements, typically 100 times smaller than the grain diameter, are exaggerated for clarity.)

3.2 DEM Simulation method

The basic geometry is equivalent to that used in the velocity correlation study in section 2.8, except that we consider a single drainage of the container, with no recycling of particles using periodic coordinates. The silo has width $50d$ and thickness $8d$ with side walls at $x = \pm 25d$ and front and back walls at $y = \pm 4d$, all with friction coefficient $\mu = 0.5$. The initial packing is generated by pouring $N = 55{,}000$ particles in from a fixed height of $z = 170d$ and allowing them to come to rest under gravity, filling the silo up to $H_o \approx 110d$. We also studied a taller system with $N = 135{,}000$ generated by pouring particles in from a height of $z = 495d$, which fills the silo to $H_o \approx 230d$. We refer to these systems by their initial height H_o. Drainage is initiated by opening a circular orifice of width $8d$ centered at $x = y = 0$ in the base of the silo ($z = 0$). A snapshot of all particle positions is recorded every 2×10^4 time steps ($\delta t = 1.75 \times 10^{-6}$ s). Once particles drop below $z = -10d$, they are removed from the simulation.

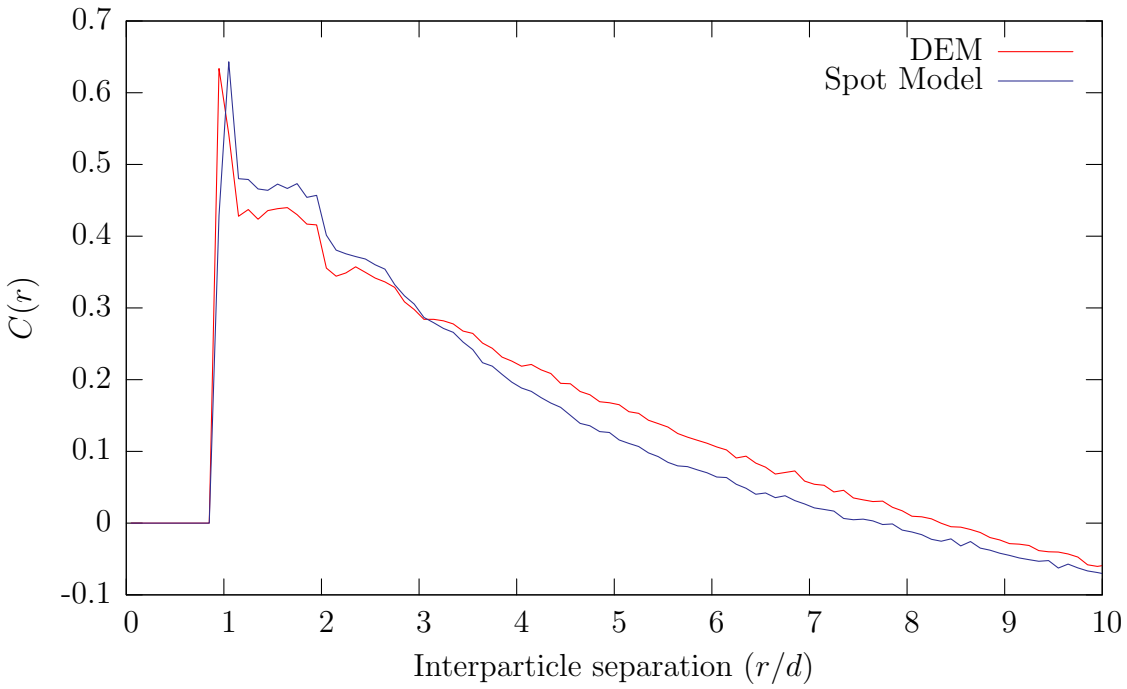

Figure 3-3: Comparison of velocity correlations calculated over the time period 0.52 s $< t <$ 1.57 s. Calculations are based on particle velocity fluctuations about the mean flow in a $16d \times 16d$ region high in the center of the container. For $H_o = 110d$.

3.3 Calibration of the model

We begin by calibrating the spot radius R_s by examining velocity correlations and comparing to the theoretical predictions of figure 2-4. The velocity correlations in the DEM simulation are shown in figure 3-3. Since the shapes of the two curves do not match, partly due to relaxation effects, we fit the simulation data to a simple decay, $C(r) = \alpha e^{-r/\beta}$ with $\beta = 1.87d$. We also fit a simple decay of the same form to the theoretical prediction, finding $\beta = 0.72R_s$, so we infer $R_s = 2.60d$ as the spot radius. Thus a grain has significant dynamical correlations with neighbors up to three diameters away.

Next, we infer the dynamics of spots, postulating independent random walks as a first approximation. We assume that spots drift upward at a constant mean speed, $v_s = \Delta z_s/\Delta t$, (determined below), opposite to gravity, while undergoing random horizontal displacements of size Δx_s in each time step Δt. The spot diffusion length, $b_s = \mathrm{Var}(\Delta x_s)/2\Delta z_s$, is obtained from the spreading of the mean flow away from the

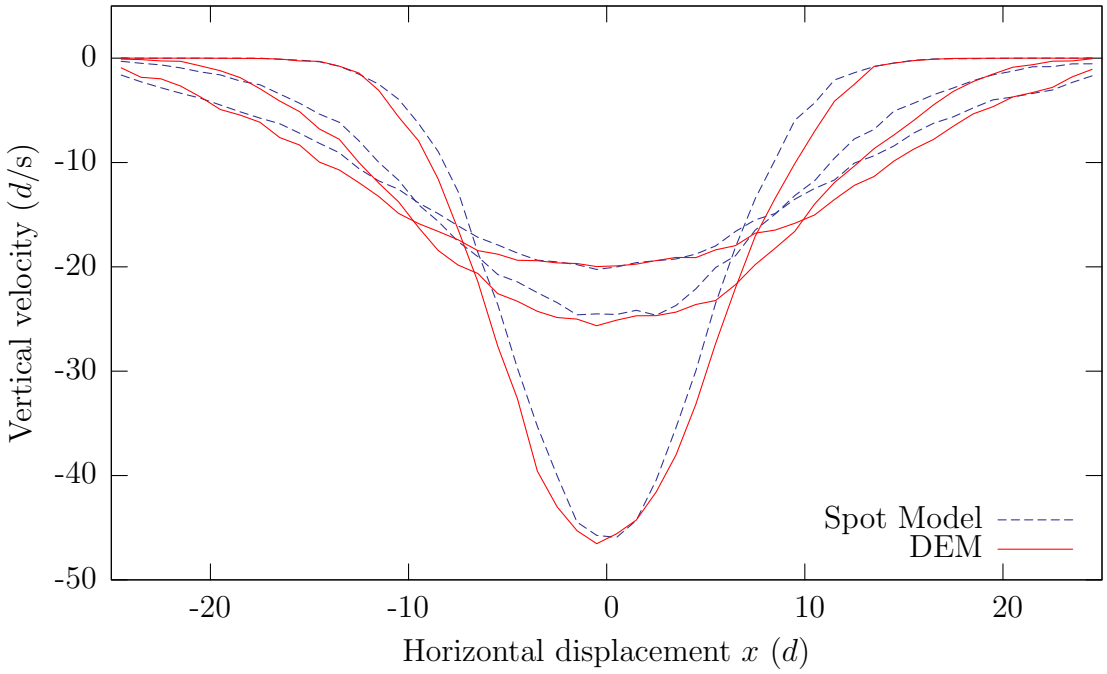

Figure 3-4: Comparison of the mean velocity profile, for three different heights calculated over the time period 4.37 s $< t <$ 5.25 s once steady flow has been established. The spot model successfully predicts a Gaussian velocity profile near the orifice and the initial spreading of the flow region with increasing height, although the DEM flow becomes more plug-like higher in the silo.

orifice. In DEM simulations, the horizontal profile of the vertical velocity component is well described by a Gaussian, whose variance grows linearly with height, as shown in Fig. 3-4. Applying linear regression gives $\mathrm{Var}(u_z) = 2.28zd + 1.60d^2$, which implies $b_s = 2.28d/2 = 1.14d$. To reproduce the spot diffusion length, we chose $\Delta z_s = 0.1d$ and $\Delta x_s = 0.68d$.

The typical excess volume carried by a spot can now be obtained from a single bulk diffusion measurement. From the previous chapter, we know that the particle diffusion length, b_p, is given by

$$b_p = \frac{\mathrm{Var}(\Delta x_p)}{2\Delta z_p} = \frac{\mathrm{Var}(w\Delta x_s)}{2w\Delta z_s} = wb_s.$$

We measure b_p in the DEM simulation by tracking the variance of the x displacements of particles that start high in the silo as a function of their distance dropped. We

find $b_p = 2.86 \times 10^{-3} d$ and thus $w = 2.50 \times 10^{-3}$. During steady flow in the DEM simulation, a typical packing fraction of particles is 57.9%, so a spot with radius $R_s = 2.60d$ influences on average 81.7 other particles. Thus we find that a spot carries roughly 20% of a particle volume: $V_s = 81.7 V_p w = 0.205 V_p$.

The three spot parameters so far (radius, R_s, diffusion length, b_s, and influence factor, w) suffice to determine the geometrical features of a steady flow, such as the spatial distribution of mean velocity and diffusion, but two more are needed to introduce time dependence. The first is the mean rate of creating spots at the orifice (for simplicity, according to a Poisson process). In the DEM simulation, particles exit a rate of mean rate of 4.40×10^3 s^{-1}, so spots carrying a typical volume $V_s = 0.205 V_p$ should be introduced at a mean rate of $\nu_s = 2.15 \times 10^4$ s^{-1}. The second remaining spot parameter is the vertical drift speed, or, equivalently, the mean waiting time between spot displacements, Δt, which can be inferred from the drop in mean packing fraction during flow. In the DEM simulation, we find that there are initially 9,400 particles in the horizontal slice, $50d < z < 70d$, which drops to 8,850 during flow. Choosing the spot waiting time to be $\Delta t = 8.68 \times 10^{-4}$ s reproduces this decrease in density in the spot simulation. The spot drift speed is thus $v_s = 0.1d/\Delta t = 115d/\text{s} = 34.5$ cm/s, which is roughly ten times faster than typical particle speeds in Fig. 3-4.

3.4 Spot model simulation

Having calibrated the five parameters (R_s, b_s, w, ν_s, v_s), we can test the spot model by carrying out drainage simulations starting from the same static initial packing as for the DEM simulations. For efficiency, a standard cell method (also used in the parallel DEM code) is adapted for the spot simulations. The container is partitioned into a grid of $10 \times 3 \times N_z$ cells, each responsible for keeping track of the particles within it, with $N_z = 30$ for $H_o = 110d$ and $N_z = 60$ for $H_o = 230d$. When a spot moves, only the cells influenced by the spot need to be tested, and particles are transferred between cells when necessary. Without further optimization, the multiscale spot simulation runs over 100 times faster than the DEM simulation.

The flow is initiated as spots are introduced uniformly at random positions on the orifice (at least R_s away from the edges) at random times according to a Poisson process of rate ν_s. (The waiting time is thus an exponential random variable of mean ν_s^{-1}.) Once in the container, spots also move at random times with a mean waiting time, $\Delta t = v_s/\Delta z_s$. Spot displacements in the bulk are chosen randomly from four displacement vectors, $\Delta\mathbf{r}_s = (\pm\Delta x_s, 0, \Delta z_s), (0, \pm\Delta x_s, \Delta z_s)$, with equal probability, so spots perform directed random walks on a body-centered cubic lattice (with lattice parameter $2\Delta z_s = 0.2d$). We make this simple choice to accelerate the simulation because more complicated, continuously distributed and/or smaller spot displacements with the same drift and diffusivity give very similar results. Spot centers are constrained not to come within d of a boundary; this distance was an arbitrary choice, and altering it allows the boundary layer velocities in the simulation to be tuned; a careful study of this issue remains a subject for future work. Once a spot reaches the top of the packing, it is removed from the simulation.

The particles in the simulation move passively in response to spot displacements without any lattice constraints. Consider a spot initially located at $\mathbf{r}_s$, being displaced by an amount $\Delta\mathbf{r}_s$. When it moves, all particles within a ball of radius R_s are displaced by an amount $-w\Delta\mathbf{r}_s$. Two different formulations were considered for the positioning of this ball:

1. Center the ball at the end of the spot displacement, at $\mathbf{r}_s + \Delta\mathbf{r}_s$
2. Center the ball at the midpoint of the spot displacement, at $\mathbf{r}_s + \Delta\mathbf{r}_s$

These two formulations are somewhat analogous to different definitions of stochastic differentials, with the first resembling the Itō formulation and the second being closer to the Stratinovich form [17, 111]. Since the diameter of the spot is larger than the spot step size, one might expect that the differences between the two approaches would be negligible in the simulation, but it turns out that it can have an important effect. The first definition is the more theoretically straightforward of the two, and also appears to be directly analogous to the void model: if a void moves from location A to location B, then the particle displacement should be centered on B. However,

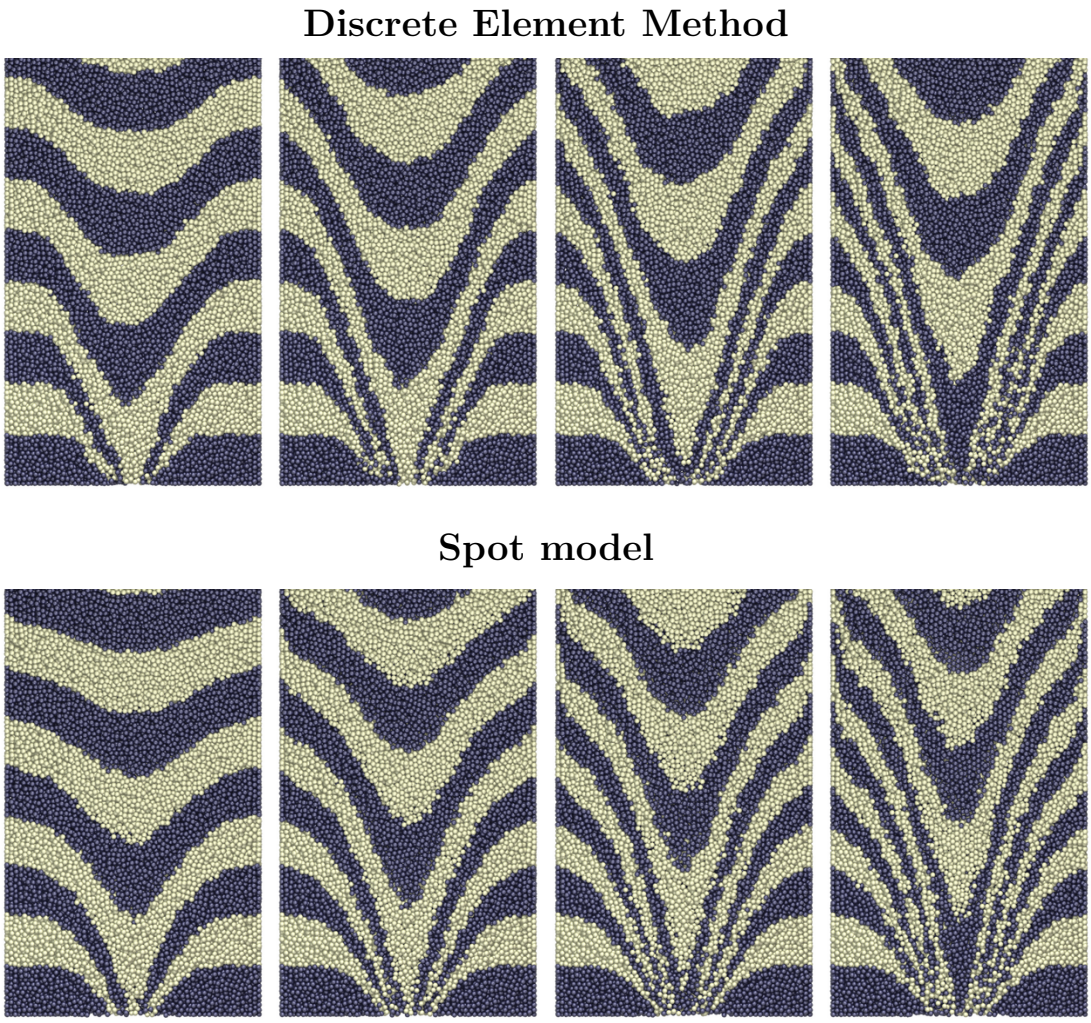

Figure 3-5: Time evolution of the random packing (from left to right) in DEM (top) and the spot simulation (bottom), for the $H_o = 230d$ system, starting from the same initial state. Each image is a vertical slice through the center of the silo near the orifice well below the free surface.

spot simulations using this method created some undesirable results, with the particles appearing to peel away from the walls.

To see why this may happen, it is helpful to consider the horizontal random walk motion of a spot. For simplicity, consider the x component of the spot motion, and assume that in this direction the spot is constrained to lie on lattice points labeled from 1 to N. Using the random walk prescription described above, we see that a spot at an internal lattice point n has a $\frac{1}{4}$ probability of moving to $n-1$, and a $\frac{1}{4}$ probability of moving to $n+1$. There is also a $\frac{1}{2}$ probability of staying at n, if the spot's motion at this step was in the y direction, leading to a zero displacement in the x direction. A spot at the boundary lattice point N has a $\frac{1}{4}$ probability of moving to $N-1$ and a $\frac{3}{4}$ probability of staying at N.

High in the container, the spots will be uniformly distributed on the N lattice sites. Particles will move rightwards if a spot at a lattice site from 2 to N moves leftwards. Using the Itō approach, the particle displacements from these spot motions will be centered on the final positions of the spots, namely lattice sites 1 to $N-1$. By a similar argument one can see that leftwards particle motion will be centered on lattice sites 2 to N. We therefore see that there is a disparity between the ranges over which the two motions are applied: rightwards particle motion occurs up to lattice site $N-1$, but leftwards motion occurs up to lattice site N. This difference causes a inward-pointing net displacement of particles near the boundary, causing them to peel away from the walls.

The Stratinovich approach resolves this problem, since both the leftwards and rightwards particle displacements are centered on the half-lattice points $1\frac{1}{2}, 2\frac{1}{2}, \ldots, N-\frac{1}{2}$. The approach is roughly analogous to thinking of a spot continuously moving from $\mathbf{r}_s$ to $\mathbf{r}_s + \Delta\mathbf{r}_s$, which continuously displaces the particles as it goes. Because of these advantages, the approach was employed for the simulations presented here. However, a more careful study of this issue is definitely needed. The above argument is specific to precise description of the random walk process, and for different spot motions, it may be that the Itō formulation is more appropriate.

To preserve realistic packings, we carry out a simple elastic relaxation after each

spot-induced block motion, as in Fig. 3-2(b). All particles within a radius $R_s + 2d$ of the midpoint of the spot displacement exert a soft-core repulsion on each other, if they begin to overlap. Rather than relaxing to equilibrium or integrating Newton's laws, however, we use the simplest possible algorithm: each pair of particles separated by less than d moves apart with identical and opposite displacements, $(d - r)\alpha$, for some constant $\alpha < 1$. Similarly, a particle within $d/2$ of a wall moves away by a displacement, $(\frac{d}{2} - r)\alpha$. Particle positions are updated simultaneously once all pairings are considered, but those within the shell, $R_s + d < r < R_s + 2d$, more than one diameter away from the initial block motion, are held fixed to prevent long-range disruptions.

It turns out that, due to the cooperative nature of spot model, only an extremely small relaxation is required to enforce packing constraints, mainly near spot edges where some shear occurs. Here, we choose $\alpha = 0.8$ and find that the displacements due to relaxation are typically less than 25% of the initial block displacement, which is at the scale of 1/10,000 of a particle diameter: $0.25w\Delta r_s \approx 2 \times 10^{-4} d$. Due to this tiny scale, the details of the relaxation do not seem to be very important; we have obtained almost indistinguishable results with $\alpha = 0.6$ and $\alpha = 1.0$ and also with more complicated energy minimization schemes. As such, we do not view the soft-core repulsion as introducing any new parameters.

3.5 Results

The spot and DEM simulations are compared using snapshots of all particle positions taken every 2×10^4 time steps. As shown in Figure 3-5, the agreement between the two simulations is remarkably good, considering the small number of parameters and physical assumptions in the spot model. It is clear *a posteriori* that the relaxation step, in spite of causing only minuscule extra displacements, manages to produce reasonable packings during flow, while preserving the realistic description of the mean velocity and diffusion in the basic spot model. Only one parameter, b_s, is fitted to the mean flow, but we find that the entire velocity profile is accurately reproduced

in the lower part of the container, as shown in Fig. 3-4, although the flow becomes somewhat more plug-like in DEM simulation higher in the container. Similarly, we fit w to the particle diffusion length in middle of the DEM simulation, $b_p = 2.86 \times 10^{-3} d$, without accounting for the elastic relaxation step, so it is reassuring that the same measurement in the spot simulation yields a similar value, $b_p = 2.73 \times 10^{-3} d$.

The most surprising findings concern the agreement between the DEM and spot simulations for various *microscopic* statistical quantities. First, we consider the radial distribution function, $g(r)$, which is the distribution of inter-particle separations, scaled to the same quantity in a ideal gas at the same density. For dense sphere packings, the distribution begins with a large peak near $r = d$ for particles in contact and smoothly connects smaller peaks at typical separations of more distant neighbors, while decaying to unity. As shown in Fig. 3-6, the functions $g(r)$ from the spot and DEM simulations are nearly indistinguishable, across the entire range of neighbors for the $H_o = 110d$ system. This cannot be attributed entirely to the initial packing because each simulation evolves independently through substantial drainage and shearing.

Next, we consider the three-body correlation function, $g_3(\theta)$, which gives the probability distribution for "bond angles" subtended by separation vectors to first neighbors (defined by separations less than the first minimum of $g(r)$ at $1.38d$). For sphere packings, $g_3(\theta)$ has a sharp peak at 60° for close-packed triangles, and another broad peak around $110 - 120^\circ$ for larger crystal-like configurations. In Fig. 3-7, we reach the same conclusion for $g_3(\theta)$ as for $g(r)$: The spot and DEM simulations evolve independently from the initial packing to nearly indistinguishable steady states.

The striking agreement between the spot and DEM simulations seems to apply not only to structural, but also to dynamical, statistical quantities. Returning to Fig. 3-3, we see that the two simulations have very similar spatial velocity correlations. Of course, the spot size, R_s, in the Spot model (without relaxation) was fitted roughly to the scale of the correlations in the DEM simulation, but the multiscale spot simulation also manages to reproduce most of the fine structure of the correlation function.

At much longer times, however, the random packings are no longer indistinguish-

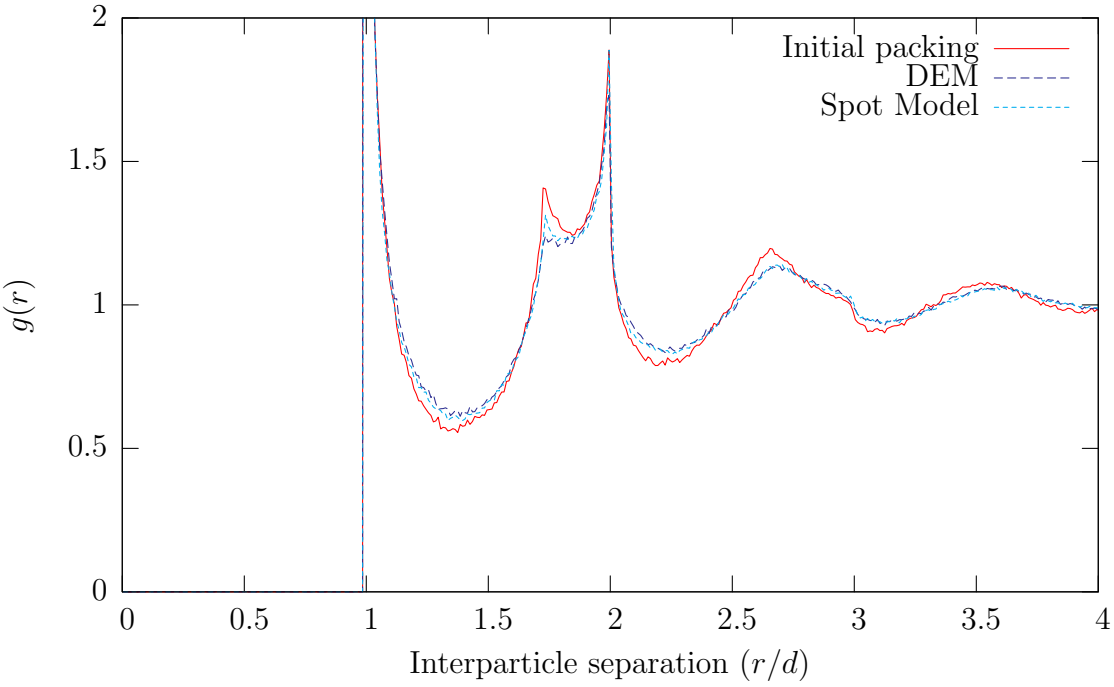

Figure 3-6: Comparison of radial distribution functions for particles in the region $-15d < x < 15d$, $15d < z < 45d$ for $H_o = 110d$ system. Three curves are shown on each graph, the first calculated from the initial static packing (common between the two simulations), and the second and third calculated for over the range 1.04 s $< t <$ 1.40 s.

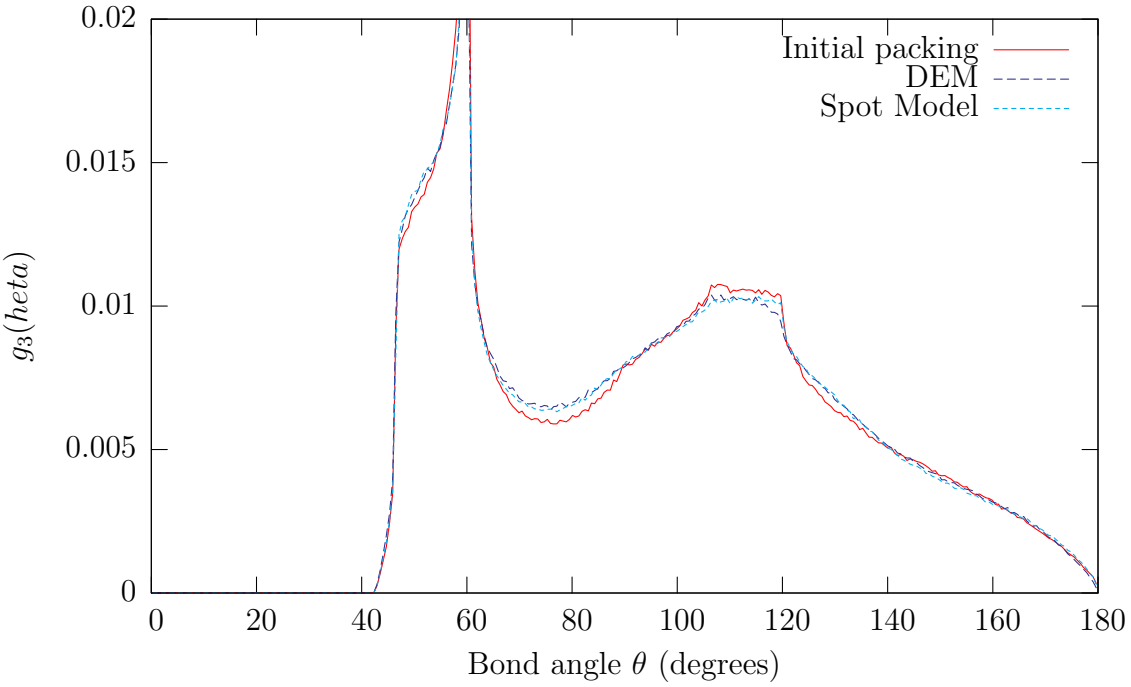

Figure 3-7: Comparison of bond angles for particles in the region $-15d < x < 15d$, $15d < z < 45d$ for $H_o = 110d$ system. Three curves are shown on each graph, the first calculated from the initial static packing (common between the two simulations), and the second and third calculated for over the range 1.04 s $< t <$ 1.40 s.

able, as a small tendency for local close-packed ordering appears the spot simulation. As shown in Fig. 3-8, the spot simulation develops enhanced crystal-like peaks in $g(r)$ at $r = \sqrt{3}d$, $2d$, ... The number of particles involved, however, is very small ($\sim 2\%$), and the effect seems to saturate, with no significant change between 8s and 16s. This is consistent with even longer spot simulations in systems with periodic boundary conditions, which reach a similar, reproducible steady state (at the same volume fraction) from a variety of initial conditions [104]. In all cases, the spot algorithm never breaks down (e.g. due to jamming or instability), and unrealistic packings with overlapping particles are never created.

The structure of the flowing steady state is fairly insensitive to various details of the spot algorithm. For example, changing the relaxation parameter (in the range $0.6 \leq \alpha \leq 1.0$), rescaling the spot size (by $\pm 25\%$), and using a persistent random walk (for smoother spot trajectories), all have no appreciable effect on $g(r)$. On the other hand, decreasing the vertical spot step size (in the range $0.025d \leq \Delta z \leq 0.1d$) tends to inhibit spurious local ordering and reduce the difference in $g(r)$ between the spot and DEM simulations (e.g. measured by the L_2 norm). Therefore, our spot algorithm appears to "converge" with decreasing time step (and increasing computational cost), analogous to a finite-difference method, although this merits further study.

3.6 Conclusions

Our results suggest that *flowing* dense random packings have some universal geometrical features. This would be in contrast to static dense random packings, which suffer from ambiguities related to the degree of randomness and definitions of jamming [134, 99]. The similar packing dynamics in spot and DEM simulations suggest that geometrical constraints dominate over mechanical forces in determining structural rearrangements, at least in granular drainage. Some form of the spot model may also apply to other granular flows and perhaps even to glassy relaxation, where localized, cooperative motion also occurs [35, 142].

The spot model provides a simple framework for the multiscale modeling of liquids

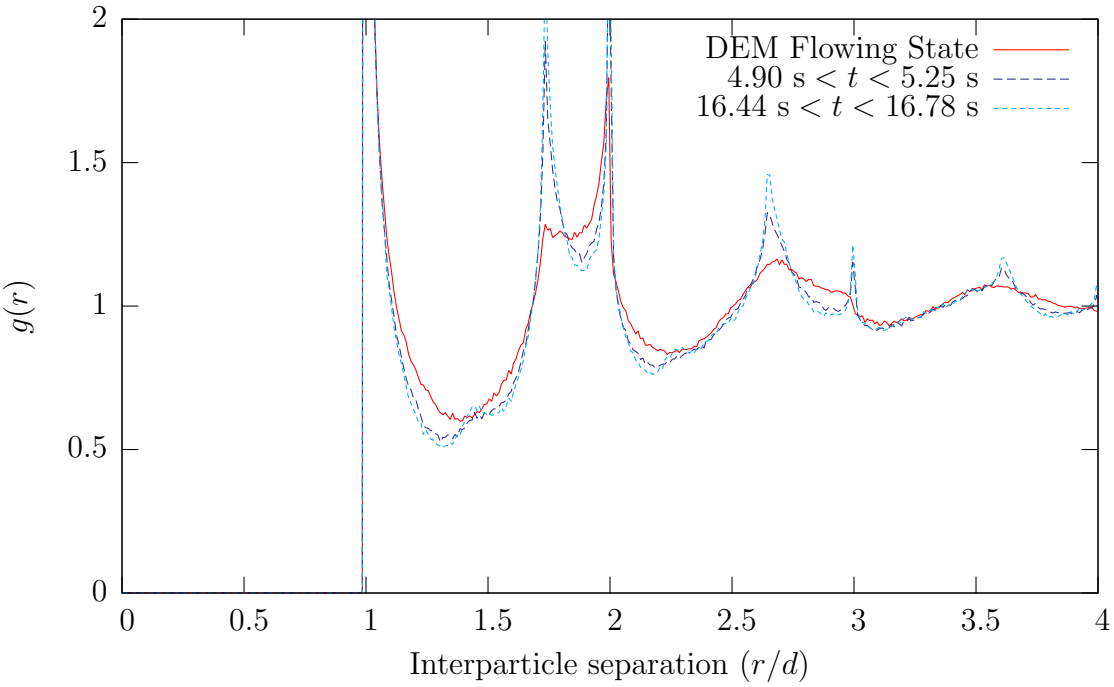

Figure 3-8: Evolution of the radial distribution function $g(r)$ for $H_o = 230d$ in the region $-15d < x < 15d$, $15d < z < 45d$. The spot simulation (dashed curves) reaches a somewhat different steady state from the DEM simulation (solid curve), after a large amount of drainage has taken place.

and glasses, analogous to dislocation dynamics in crystals. Our algorithm, which combines an efficient, "coarse-grained" simulation of spots with limited, local relaxation of particles, runs over 100 times faster than fully particle-based DEM for granular drainage. On current computers, this means that simulating one cycle of a pebble-bed reactor [130] can take hours instead of weeks, although a general theory of spot motion in different geometries is still lacking. In any case, we have demonstrated that dense random-packing dynamics can be driven entirely by the motion of simple, collective excitations.